



ELSEVIER

Catalysis Today 48 (1999) 119–124



Mass transfer resistances in the palladium-catalysed hydrogenation of 1-methoxy-2,4-(nitrophenyl)-ethane

Tatjana Glavanović^{a,*}, Stanka Zrnčević^b

^aPliva-Research Institute, Zagreb, Croatia

^bFaculty of Chemical Engineering and Technology, Zagreb, Croatia

Abstract

Hydrogenation of 1-methoxy-2,4-(nitrophenyl)-ethane (MNPE) to 1-methoxy-2,4-(aminophenyl)-ethane (MAPE) over Pd/C catalyst was studied in a three-phase stirred slurry reactor. The reaction was performed in a kinetic region (no internal and external mass transfer resistances) at temperatures ranging from 293 to 320 K, hydrogen pressure 200 kPa using powdered pellets of 1–4% Pd on carbon support. The rates have been correlated with power law and Hougen–Watson kinetic models. The rate expression which best fit the data is

$$r_B = \frac{k_1 C_A C_B}{1 + K_B C_B},$$

which postulates a reaction between adsorbed MNPE (marked by B) and hydrogen (marked by A). © 1999 Elsevier Science B.V. All rights reserved.

Keywords: Hydrogenation; Specially chemicals; Catalyst preparation; Multiphase reactor

1. Introduction

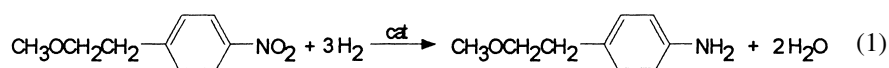
Catalytic hydrogenation of nitro compounds to amine in the liquid phase is important in a great variety of chemical processes for fine chemicals, pharmaceuticals and agrochemicals. Commonly, for the catalytic hydrogenation of nitro substituted aromatic compounds, Pd, Pt and Ni are used as catalysts.

Often the reaction rates found are the zero order in the nitro compound and between zero and one in hydrogen [1–3]. In general, the nitro compounds are

converted to the amine quantitatively which depend on catalyst activity and selectivity [4–6].

These reactions are generally carried out in mechanically agitated slurry reactors in which gas–liquid, liquid–solid and intraparticle diffusional resistances are likely to exist. For the purpose of kinetic study, it is important to ensure that the rate data are obtained under kinetically controlled regime or the contribution of the mass transfer is suitably incorporated.

Considering the industrial significance of multiphase hydrogenation MNPE to MAPE, described as



*Corresponding author.

a detailed investigation on catalysis and kinetic modelling was undertaken in this work.

2. Experimental

The hydrogenation experiments were carried out in a stirred batch autoclave reactor supplied by Parr Instrument of 0.2 dm³. Fig. 1 shows a schematic diagram of the experimental set-up.

This reactor was provided with automatic temperature control arrangement for sampling of liquids and variable agitation speeds. In a typical hydrogenation experiment known quantities of MNPE and solvent methanol were charged into the reactor stirred for half an hour and heated to a desired temperature. After the catalyst was added to the reactor the content was stirred in order to pretreat the Pd/C with reactant. Then, the reactor was flushed with hydrogen and pressurised to a desired level. The instant that the pressure was achieved was assumed to be the start (time=0) of the reaction.

The liquid samples were also withdrawn at different time intervals to analyse reaction mixture. The analysis of the liquid samples was carried out using a gas

chromatography with 3% OV17 succinate on 80/100 mesh Chromosorb W HP DMCS. In addition to the routine analysis, some samples have been analysed by GC-MS. The catalyst used for hydrogenation of MNPE was Pd/C with different surface activity (1–4%) obtained by precipitation [7]. The physical properties of the catalysts are surface area of 8×10^4 dm² g⁻¹, pore volume of 1.84×10^4 dm³ g⁻¹ and average particle size 1.6×10^{-4} dm. The initial MNPE concentration was 3.36×10^{-3} mol dm⁻³, hydrogen pressure 200 kPa and the temperature was between 293 and 320 K.

3. Results and discussion

In order to analyse the contribution of mass-transfer steps on rate of MNPE, hydrogenation method was suggested by Gholap et al. [8].

The hydrogenation of MNPE to MAPE over Pd/C catalyst is known to be first-order with respect to the hydrogen pressure [7]. The rate of reaction in a multiphase reactor for the case of first-order reaction is given by the following equation [8]:

$$\frac{c_A^*}{r_{A0}} = \frac{1}{k_1 a_b} + \frac{1}{w} \left[\frac{\rho_p d_p}{6k_s} + \frac{1}{P_0 \eta k} \right]. \quad (2)$$

In a series of runs in which the Pd content P_0 is varied but the catalyst loading w and the particle size d_p are the same, the reciprocal of the reaction rate c_A^*/r_{A0} should be linear in $1/P_0$ (see Fig. 2).

The intercept of the plots in Fig. 1 is equal to the external mass-transfer resistance. Values of the intercept observed at different catalyst loading were plotted as I versus $1/w$ as shown in Fig. 3.

From the intercept $k_1 a_b$ was 0.16 min^{-1} . Then determining the slope of the resulting straight line in Fig. 3 and from knowledge of ρ_p and d_p , liquid-solid mass-transfer coefficient k_s was determined to be 2.12 dm min^{-1} .

Further, factors α_1 , α_2 and ϕ which are defined as the ratios of the maximum rates of gas-liquid, liquid-solid and intraparticle mass-transfer rates were calculated [9]. This analysis showed that the values of α_1 , α_2 and ϕ for the data at all concentrations of Pd (1–4%) and all catalyst loadings (0.326 – 0.100 g dm^{-3}) were between 0.010 and 0.114, 0.001 and 0.052, and 0.05 and 0.08, respectively. This provides a rough indi-

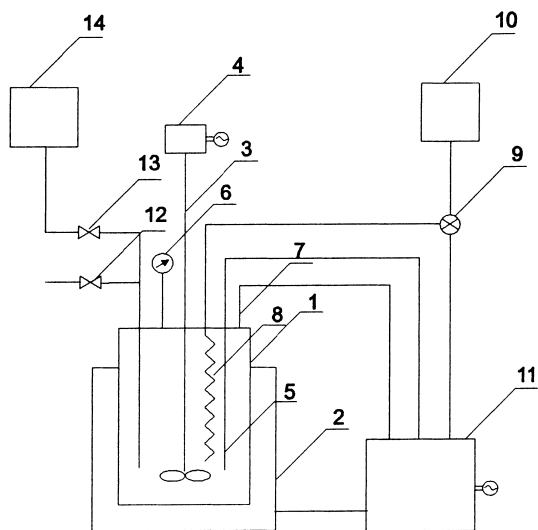


Fig. 1. Experimental set-up: (1) reactor; (2) heater; (3) stirrer; (4) motor; (5) thermocouple; (6) pressure indicator, 0–3000 psi; (7) pressure transducer; (8) cooling loop; (9) cooling supply solenoid valve; (10) cooling water source; (11) temperature controller with motor speed control; (12) sampling valve; (13) H₂ inlet; (14) H₂ cylinder.

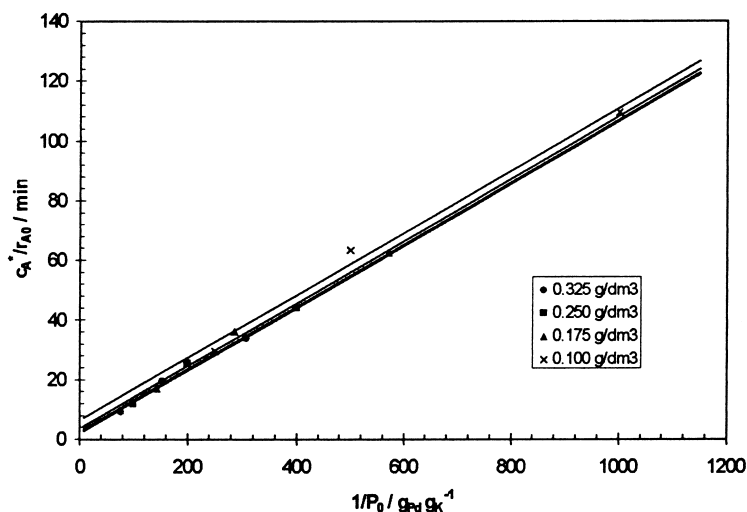


Fig. 2. Plot of c_A^*/r_A versus $1/P_0$ for different catalyst loadings (agitation speed=1100 rpm, hydrogen pressure=200 kPa, MAPE concentration= 3.36×10^{-3} mol dm $^{-3}$, and temperature=313 K).

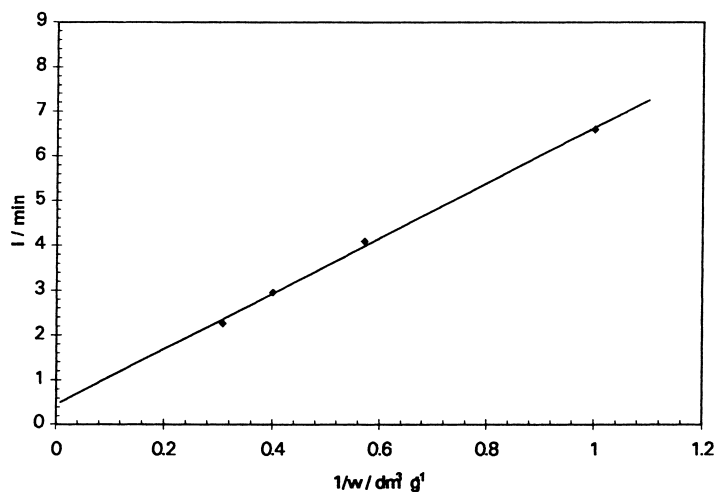
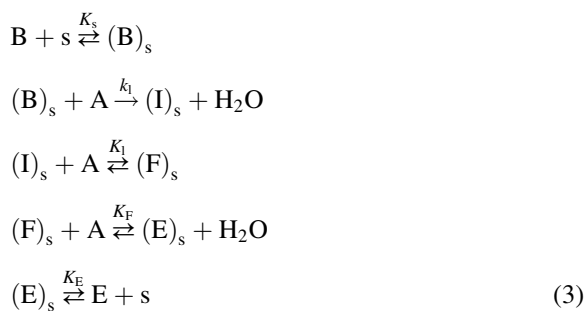


Fig. 3. Plot of intercepts versus $1/w$ (agitation speed=1100 rpm, hydrogen pressure=200 kPa, MAPE concentration= 3.36×10^{-3} mol dm $^{-3}$, and temperature=313 K).

cation that external and internal mass-transfer resistances do not affect the rate of MNPE hydrogenation.

To study the reaction pathway, hydrogenation experiments have been performed at constant reactor pressure 200 kPa, at temperature ranging from 293 to 320 K and at different catalyst activity (1–4% Pd). The results suggest that the direct route to an amine goes via corresponding nitroso and hydroxyl compound [10] which is consistent with the following reaction scheme:



where I and F represent intermediate (nitroso and hydroxyl compound) and E represent the product MAPE. Assuming that the reaction between adsorbed MNPE and hydrogen is the rate controlling step, the rate Eq. (4) can be derived. If we presume that the intermediates I and F are very reactive then Eq. (4) can be simplified as Eq. (5):

$$r_B = \frac{k_I K_B c_A c_B L}{1 + c_E / K_E + c_{ECH_2O} / K_F K_E c_A + C_{ECA} / K_I K_F K_E c_A + c_B K_B}, \quad (4)$$

$$r_B = \frac{k_I c_A c_B}{1 + K_B c_B}. \quad (5)$$

In order to evaluate the rate parameters in the above equation, the observed concentration–time data were simulated using a batch reactor model. For constant hydrogen pressure and isothermal conditions used in this work the material balance equation is

$$-\frac{dc_B}{dt} = r_B \quad (6)$$

with the initial conditions that at $t=0$, $c_B=c_{B_0}$.

The parameters were determined with nonlinear regression using the software Scientist. The residual sum of squares calculated from the differences between experimental and predicted concentrations was minimised in the regression.

Some typical results that illustrate the comparison of the model predictions with experimental data are given in Figs. 4–6.

Figs. 4–6 show that with increasing concentration of catalytic active sites, catalyst loading and reactor temperature rate of hydrogenation increase. But at temperature exceeding 320 K catalyst selectivity

decreases because of hydrogenation of methoxy group in aromatic ring.

The temperature dependence of the rate constants is shown in Fig. 7, from which the activation energy was calculated as 28.3 kJ mol^{-1} and is in accordance with the data for aromatic compounds hydrogenation [11,12].

4. Conclusions

Hydrogenation of MNPE on Pd/C catalyst has been studied using a batch slurry reactor. For the purpose of kinetic analysis some experiments were conducted in order to select the range of operating conditions where no diffusional limitations exist.

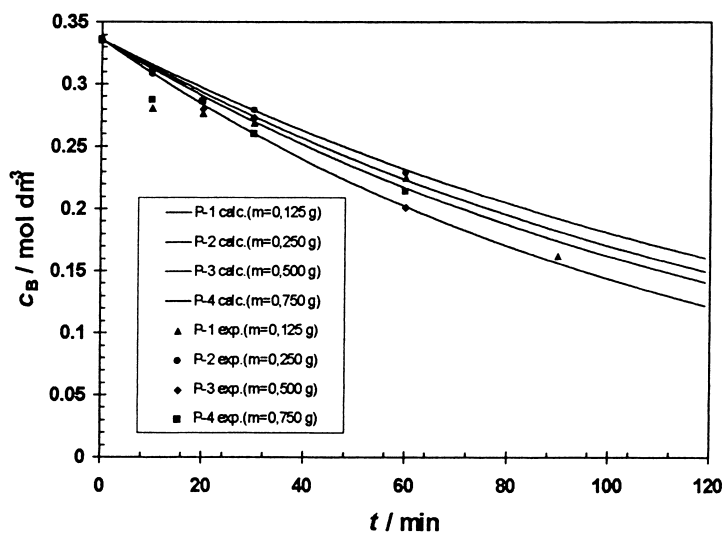


Fig. 4. Effect of catalyst loading on MNPE hydrogenation (temperature=313 K, agitation speed=1100 rpm, hydrogen pressure=200 kPa, and Pd content=4%).

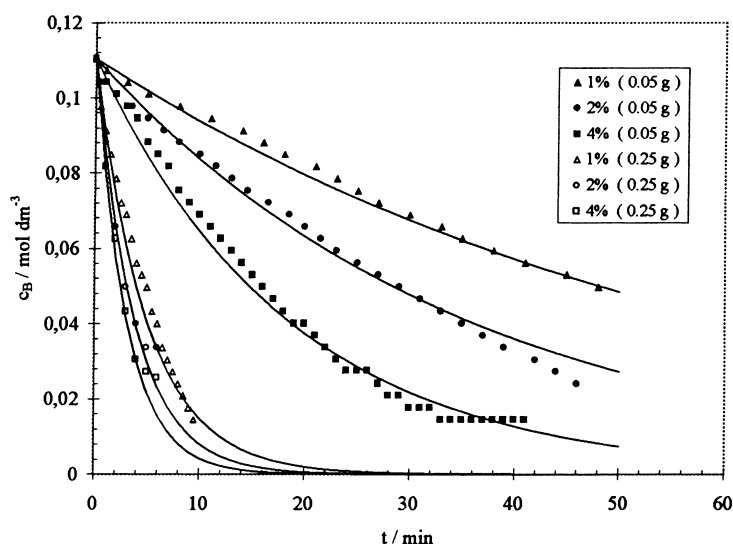


Fig. 5. Effect of Pd concentration on MNPE hydrogenation (temperature=313 K, agitation speed=1100 rpm, and hydrogen pressure=200 kPa).

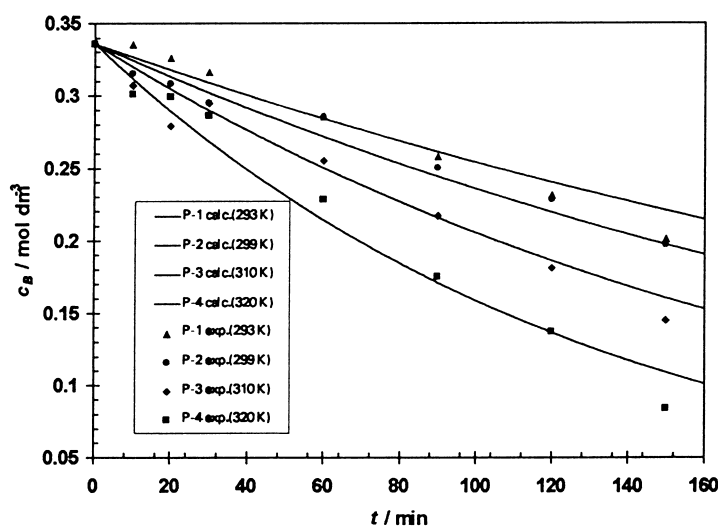


Fig. 6. Effect of temperature on MNPE hydrogenation (agitation speed=1100 rpm, hydrogen pressure=200 kPa, and Pd content=4%).

In the range of the operation conditions, MNPE is converted to MAPE via two reactive nitroso and hydroxy compound intermediate according to the Haber reaction scheme. A kinetic model was developed to predict the concentration–time profile. The predicted and observed results were found to agree very well.

5. Nomenclature

- a_b surface area of bubbles per unit volume of bubble (dm^{-1})
- c_A concentration of hydrogen (mol dm^{-3})
- c_B concentration of MNPE (mol dm^{-3})
- d_p particle diameter (dm)

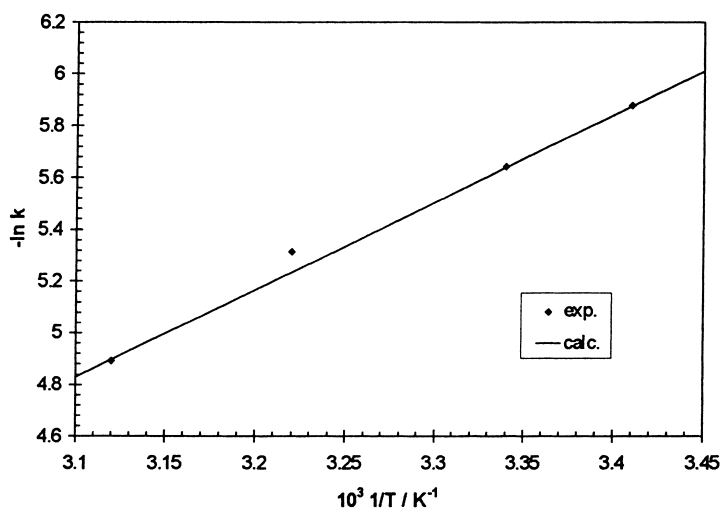


Fig. 7. Temperature dependence of hydrogenation rate constants (agitation speed=1100 rpm, hydrogen pressure=200 kPa, MAPE concentration= 3.36×10^{-3} mol dm $^{-3}$, catalyst loading=0.25 g, and Pd content=4%).

k	rate coefficient (min $^{-1}$)
k_l	transfer coefficient gas–liquid (dm min $^{-1}$)
k_s	transfer coefficient liquid–solid (dm min $^{-1}$)
L	total number of sites
m	mass of catalyst (g)
P_0	palladium concentration (g _{Pd} g $^{-1}$)
r_B	reaction rate (mol dm $^{-3}$ min $^{-1}$)
t	time (min)
w	mass of catalyst per unit volume (g dm $^{-3}$)
ρ_p	effective density of catalyst (g dm $^{-3}$)
ϕ	pore diffusion modulus
η	effectiveness factor

References

- [1] H.J. Jansen, A.J. Kruithof, G.J. Steghuis, K.R. Westerterp, *Ind. Eng. Chem. Res.* 29 (1990) 1822.
- [2] H.J. Janssen, A.J. Kruithof, G.J. Steghuis, K.R. Westerterp, *Ind. Eng. Chem. Res.* 30 (1990) 1456.
- [3] C.V. Rode, R.V. Chaudhari, *Ind. Eng. Chem. Res.* 33 (1994) 1645.
- [4] G.J.K. Acres, B.J. Cooper, *J. Appl. Chem. Biotechnol.* 22 (1972) 769.
- [5] H.D. Burge, D.J. Collins, B.H. Davis, *Ind. Eng. Chem. Prod. Res. Dev.* 19 (1980) 389.
- [6] D.J. Collins, A.D. Smith, *Ind. Eng. Chem. Prod. Res. Dev.* 21 (1982) 279.
- [7] T. Glavanović, M. Durinski, S. Zrnčević, *Chem. Biochem. Eng. Q.* 10 (1996) 49.
- [8] R.V. Gholap, D.S. Kolhe, R.V. Chaudhari, G. Emig, H. Hofmann, *Chem. Eng. Sci.* 42 (1987) 1689.
- [9] P.A. Ramahandran, R.V. Chaudhari, *Three Phase Catalytic Reactors*, Gordon and Breach, New York, 1983.
- [10] F. Haber, *Z. Elektrochem.* 22 (1898) 506.
- [11] R.V. Chaudhari, R. Joganathan, D.S. Kolhe, *Appl. Chem.* 29 (1987) 141.
- [12] V.R. Chandrashekar, R.V. Chaudhari, *Ind. Eng. Chem. Res.* 33 (1994) 1645.